The Cryosphere Discuss., 7, 343–371, 2013
www.the-cryosphere-discuss.net/7/343/2013/
doi:10.5194/tcd-7-343-2013

The Cryosphere Discussions

Surface motion of active rock glaciers in the Sierra Nevada, California, USA: inventory and a case study using InSAR

Lin Liu[1], C. I. Millar[2], R. D. Westfall[2], and H. A. Zebker[1]

[1]Department of Geophysics, Stanford University, Stanford, CA, USA
[2]USDA Forest Service, Pacific Southwest Research Station, Albany, CA, USA

Received: 27 December 2012 – Accepted: 2 January 2013 – Published: 23 January 2013

Correspondence to: Lin Liu (liulin@stanford.edu)

Published by Copernicus Publications on behalf of the European Geosciences Union.

Abstract

Despite the abundance of rock glaciers in the Sierra Nevada of California, USA, few efforts have been made to measure their surface flow. Here we use the interferometric synthetic aperture radar (InSAR) technique to compile a benchmark inventory describing the kinematic state of 59 active rock glaciers in this region. Statistically, these rock glaciers moved at speeds range from 15 $cm\,yr^{-1}$ to 88 $cm\,yr^{-1}$ with a mean value of 55 $cm\,yr^{-1}$ in the late summer of 2007. We also find a spatial gradient: rock glaciers in the southern Sierra Nevada moved faster than the ones in the central Sierra Nevada. In addition to the inventory mapping, we also conduct a case study to measure the surface flow of the Mount Gibbs rock glacier in fine spatial and temporal detail. The InSAR measurements over this target reveal (1) that the spatial pattern of surface flow is influenced by surface geomorphological features and (2) a significant seasonal variation of flow speed whose peak value was 48 $cm\,yr^{-1}$ in the fall, more than twice the minimum value observed in the spring. The seasonal variation lagged air temperatures by three months and likely results from temporal changes in mechanical strength of mixing debris and ice, internal melting of ice, and surface snow cover. Our finding on the seasonal variation of surface speed reinforces the importance of a long time series with high temporal sampling rates to detect possible long-term changes of rock glaciers in a warming climate.

1 Introduction

Rock glaciers are tongue- or lobate-shaped landforms on high mountain slopes, typically consisting of mixtures of unconsolidated rock debris and ice. Rock glaciers are of geomorphological, climatic, and hydrological importance in alpine periglacial environments. They are visible indicators of permafrost and contribute to a major portion of mass transport of the alpine landforms (Barsch, 1977; Humlum, 2000; Brenning, 2005; Degenhardt, 2009). In addition, they preserve a long geological history in ice records

TCD
7, 343–371, 2013

and thus provide information and insights on paleoclimate (Clark et al., 1994; Humlum, 1998; Haeberli et al., 1999; Konrad et al., 1999; Harrison et al., 2008). Finally, they prolong ice melt and sustain surface runoff in a warming climate, acting as water reserves that are especially important in semi-arid mountain areas (Burger et al., 1999; Brenning, 2005; Croce and Milana, 2002; Millar et al., 2012).

Surface kinematics is a fundamental physical state of rock glaciers. Active rock glaciers creep downslope cohesively as a consequence of the deformation of internal ice. Surface flow is related to regional forcing including climatic conditions and local factors such as thickness, slope, and internal structures. Therefore, temporal variation in surface kinematics sheds light into changes in regional and local conditions.

Possible change of rock glacier flow in response to ongoing climate warming is also an intriguing and important problem. Compared to ice glaciers, rock glaciers are believed to be less sensitive to rising temperature due to isolation of rock mantles (Clark et al., 1994; Barsch, 1996). However, there are also emerging observations suggesting that rock glaciers in the European Alps have increased flow rates since circa 1990 (e.g. Kääb et al., 1997; Krainer and Mostler, 2000; Delaloye et al., 2008; Nöetzli and Vonder Müehll, 2010).

Both field and remote sensing methods have been used to measure rock glacier surface flow. Repeat geodetic surveys map surface displacement at selected ground markers, usually a few years apart (e.g. Wahrhaftig and Cox, 1959; Barsch, 1996; Berthling et al., 1998; Konrad et al., 1999; Lambiel and Delaloye, 2004). Due to the remote locations of rock glaciers in high mountains, field observations are usually scarce and do not provide a complete view of rock glacier movement and processes. Remote sensing techniques such as repeat photogrammetry (e.g. Kääb et al., 1997; Kääb, 2002) and terrestrial laser scanning (Avian et al., 2009) have proved to be especially useful to fill the spatial gaps.

In contrast to optical sensors, microwave interferometric synthetic aperture radar (InSAR) measures ground deformation day-or-night in all weather conditions. The spatial extent of many space-borne SAR images is approximately 100 km wide and several hundreds of km long. And most InSAR deformation maps have a spatial resolution as fine as 10 m. These merits make InSAR a unique tool for measuring rock glaciers flow kinematics including (1) inventory mapping and (2) detailed case studies on individual rock glaciers. The latter capability has been demonstrated at targets around the world (Rott and Siegel, 1999; Nagler et al., 2002; Rignot et al., 2002; Kenyi and Kaufmann, 2003; Strozzi et al., 2004).

In this study we use the InSAR technique to map surface motion of rock glaciers in the Sierra Nevada of California, USA. Despite their abundance in this region, rock glaciers are largely overlooked. They have been recently brought to wider attention partly thanks to the inventory compiled by Millar and Westfall (2008) based on their field studies (hereafter referred to as the "MW database", which is available at the National Snow and Ice Data Center http://nsidc.org/data/ggd652.html). Still, little is known about their kinematic states, let alone the long-term changes in surface flow.

Our first objective is to conduct a quantitative and nearly spatially-complete assessment on the kinematic behaviors of the active rock glaciers in the Sierra Nevada. Using space-borne InSAR data, we compile a georeferenced inventory to describe flow speed, aspect direction, and area of active motion of active rock glaciers in the region. To our knowledge, this is the first InSAR study on rock glaciers in the Sierra Nevada. Our regional-scale mapping effort on rock glaciers is the only one outside the Swiss Alps (Delaloye et al., 2010). Regional survey is difficult to accomplish logistically by field measurements. As a secondary product of the InSAR study, we are also able to identify rock glaciers based on their distinct kinematic behaviors from stable surroundings. Some of these rock glaciers have been overlooked in field studies due to their remoteness and their similar appearance to moraines and scree slopes (Millar and Westfall, 2008). For the latter reason, it is also difficult to spot many rock glaciers on optical remote sensing images.

Our second objective is to focus on a single target, the Mount Gibbs rock glacier, to image its surface motion at a fine spatial resolution and investigate its seasonal variation. Previous remote-sensing studies, including InSAR, only provided a single

TCD
7, 343–371, 2013

snapshot of surface motion over periods ranging from one day to a few years. Our case study on the Mount Gibbs rock glacier for the first time detects a significant seasonal variability of surface motion from space.

2 Rock glaciers in the Sierra Nevada of California

2.1 Overview

The Sierra Nevada is a major mountain range located between the Central Valley and the Basin and Range province in California. It has warm Mediterranean and semi-arid climates, characterized by warm dry summers and cool wet winters. The entire region was heavily glaciated during the Pleistocene (Clark and Gillespie, 1997). A few small ice glaciers and persistent snow fields are scattered at cirques in the high mountains. The glaciers are of Late Holocene origin and not relicts from the Pleistocene. Decomposed rock is abundant, especially along metamorphic exposures of the eastern escarpment.

Rock glaciers and related landforms are common throughout cirques and valleys of the central and southern parts of the range. Our study area extends from north of Bridgeport to Lone Pine as shown in Fig. 1. Millar and Westfall (2008) mapped more than 280 rock glaciers in this area. According to their different locations, origins, and shapes, Millar and Westfall (2008) further grouped the rock glaciers into two classes: cirque rock glaciers and valley wall rock glaciers. Cirque rock glaciers originate in high cirques and flow parallel to the valley axis as long-lobed debris bodies. They often have an ice or snow field at the cirque wall and arcuate flow lines on the debris surface. The MW database lists 184 cirque rock glaciers, 67 % of which are active and have a mean elevation of 3390 m and a mean size of 20 ha. Valley wall rock glaciers occur on valley walls and are characterized by wide wedge-shaped structures. The MW database includes 105 valley rock glaciers, 61 % of which are active and have a mean elevation of 3292 m and a mean size of 3 ha, much smaller than the cirque rock glaciers.

TCD
7, 343–371, 2013

2.2 Mount Gibbs rock glacier

The Mount Gibbs rock glacier is centered at 37°53′44″ N, 119°12′13″ W and is located in Gibbs Canyon along the eastern escarpment of the Sierra Nevada. Its ground and aerial photos are shown in Figs. 2 and 4a, respectively. This tongue-shaped rock glacier is approximately 700 m long in its flow direction and 300 m wide. Its geometry suggests that the rock glacier flows downslope initially in a NNE direction and then bends toward the NE and ENE. Its head is a bowl-shaped cirque wall surrounded by Mount Gibbs (3893 m a.s.l.) and Mount Dana (3980 m a.s.l.). A small ice glacier is perched in the adjacent and hanging cirque to the east of the rock glacier. Complex meta-volcanic and meta-sedimentary rocks form mountains of this region (Kistler, 1966). The rock glacier surface is covered by angular and poorly-sorted graywackes that are gray-colored meta-sedimentary rocks. Transverse furrows and longitudinal ridges are visible along two lobes in the middle and lower parts. The terminus of the rock glacier is an over-steepened face and forms the southwest shore of Kidney Lake. The till flowing into lake origins from the ice glacier at the peak of Mount Gibbs.

We choose the Mount Gibbs rock glacier for a detailed kinematic study due to several reasons. Although it is similar to other active cirque rock glacier in the MW database in elevation and size, the Mount Gibbs rock glacier has a complex geometry and thus an interesting target for mapping surface flow at fine spatial resolution. From the perspective of InSAR processing (see more in Sect. 3.2), this rock glacier is ideal because of its NE flow direction, moderate flow speed, and large debris-covered area. Practically, radar images from two satellite tracks were acquired continuously over this rock glacier (see Sect. 3.1), making a detailed time series study possible.

3 Methods

In this section, we first present technical details of InSAR processing for the case study on the Mount Gibbs rock glacier in Sect. 3.1. Then we describe a similar but simplified

TCD
7, 343–371, 2013

strategy for the regional survey and also list criteria for including an active rock glacier in our inventory in Sect. 3.2.

3.1 InSAR data and processing for case study

For the case study on the Mount Gibbs rock glacier, we apply InSAR processing using a motion-compensation strategy (Zebker et al., 2010) to the Phased Array type L-band Synthetic Aperture Radar (PALSAR) data acquired by the Japanese Advanced Land Observing Satellite (ALOS). By measuring phase differences between two radar images taken at different times, InSAR constructs an interferogram that shows ground surface displacement along the line-of-sight (LOS) direction during the time interval of the two images. To maximize the temporal sampling rates of ground deformation from spring 2007 to spring 2008, we use the PALSAR data acquired along two ascending paths: Path 216/Frame 750 and Path 217/Frame 740. Unfortunately, no descending path PALSAR scenes were acquired by the ALOS satellite over this area. We take spatial average of every two pixels in the azimuth direction on each interferogram to achieve a ground resolution of approximately 10 m by 10 m. Accordingly, we use a 10-m digital elevation model (DEM) from the USGS National Elevation Database (Gesch et al., 2002) to remove the topographic contribution. We produce a total of 12 interferograms and list them in Table 1. All interferograms have a short time span as we want to minimize InSAR phase decorrelation due to fast ground motion and to better detect seasonal variability of ground motion. The repeat orbit cycle of the ALOS satellite limits the shortest time span to 46 days. We use the SNAPHU software (Chen and Zebker, 2002) for phase unwrapping, i.e. reconstructing the absolute phase from the InSAR observable: the 2π modulus of the absolute phase. We also choose a reference point (37°54′0′ N, 119°11′44″ W) outside the rock glacier where we assume zero displacement.

To determine the ground surface motion, we project the InSAR-measured LOS displacements onto the downslope direction assuming that surface-parallel flow follows the steepest slope direction on the rock glacier surface. The InSAR LOS vector is determined by two angles: the heading angle of satellite flight path, denoted as α, and the incidence angle θ_{inc} (i.e. the angle between the incident radar waves and the direction normal to the ground surface). Along both paths, the heading angles are the same 13.5° counter-clockwise from north. Within the rock glacier area, the incidence angles are 37.5° and 40.3° for Paths 216 and 217, respectively. We use the DEM to calculate local slope angle θ_{slp} and azimuth angle β and then use the following mapping function to convert the LOS displacement (D_{LOS}) to the downslope displacement (D):

$$D = \frac{D_{LOS}}{\sin(\alpha - \beta)\sin\theta_{inc}\cos\theta_{slp} + \cos\theta_{inc}\sin\theta_{slp}}. \quad (1)$$

For each interferogram, we divide the InSAR-estimated downslope displacement by the time interval and obtain the annual equivalent speed.

We also calculate time series of surface speed at selected high coherence points. From each set of geocoded interferograms grouped according to their paths, we use the small baseline subset inversion method (Berardino et al., 2002) to estimate surface speed during two consecutive acquisition times. We then combine these two sets of speed estimates to obtain a continuous time series from spring 2007 to spring 2008. Because the tropospheric artifacts are uniform within this small area, we do not apply any atmospheric filtering in the time series inversion.

3.2 Inventory mapping using InSAR

For regional mapping, we spot the rock glaciers by a manual inspection. Instead of time series analysis using multiple interferograms, we only construct one interferogram from each ALOS PALSAR frame (roughly 100 km by 70 km). Our study area (Fig. 1) is approximately 240 km by 150 km and is completely covered by five frames: Frames 720, 730, and 740 in Path 216 and Frames 740 and 750 in Path 217. For each frame in Path 216, we construct one interferogram by applying the same InSAR processing methods described in Sect. 3.1 to the PALSAR data acquired on 18 August 2007 and 3 October 2007. Similarly for Path 217, we construct one interferogram for each frame using the data acquired on 4 September 2007 and 20 October 2007. Figure 3a shows a portion of the Path 216/Frame 730 interferogram as an example that reveals moving rock glaciers standing out from surrounding landforms. For comparison, we also show optical images taken in the summer of 1999 in Fig. 3b–d, in which rock glaciers appear similar to their surroundings.

Constrained by the capability of InSAR for mapping small targets in mountain areas, there are a few limitations on the size, flow speed, and location of a rock glacier to be included in our inventory. First, InSAR can only measure surface flow over the debris-covered area where the interferometric coherence is sufficiently high. Decorrelation in interferometry phase is common at the head due to fast motion of glacier ice. Second, the debris-covered area of a rock glacier must be larger than 2 ha to be reliably identified. For instance, the Fig. 3a interferogram barely resolves surface motion over the small rock glacier outlined by the red box in Fig. 3c. Third, at each rock glacier, the displacement component of the total phase must be significantly larger than decorrelation noise, here assumed 1 cm. For a 46-day-span interferogram, this lower bound on the flow speed is equivalent to 10 cm yr^{-1}. Fourth, we are unable to map any rock glaciers located within the radar shadow and layover zones that facing the radar illumination. In the viewing geometry of ascending frames used in this study, layover zones are on the western slopes and appear as bright stripes (outlined by the dashed white lines in Fig. 3a). Lastly, also limited by the viewing geometry, we are unable to identify any rock glaciers moving parallel to the satellite flight direction using the conventional cross-track InSAR technique. This is likely the reason that the rock glacier outlined by the red box in Fig. 3d appears not moving in the interferogram and thus is excluded in our inventory.

For each identified active rock glacier, out inventory lists the size, flow speed and aspect direction based on the InSAR measurements and the elevation based on the DEM. Similar to the Mount Gibbs rock glacier study, we choose a local reference point near but outside each rock glacier to calibrate the flow speed measurements. Using the geocoded interferograms, we measure the dimensions along and across flow direction of each active rock glacier, whose area is not always the same as the area of apparently active moraines shown on optical images. Similar to the Mount Gibbs rock glacier study, the InSAR-mapped LOS displacement is converted to downslope displacement using Eq. (1), except that we assume an incidence angle of 38° and a surface slope of 15° for all rock glaciers. We use the equivalent annual speed at the center of each rock glacier to represent its kinematic state.

4 Results

4.1 Regional inventory

Our database describes the kinematic states of 59 active rock glaciers in central and southern Sierra Nevada. Their size and surface flow speed in the late summer of 2007 are plotted in Fig. 1. We provide the complete inventory in the Supplement, including a Google Earth KMZ file and a spreadsheet of rock glacier location, elevation, size, flow speed and aspect direction. Table 2 summarizes their mean values. The mean flow speed was 55 $\mathrm{cm\,yr^{-1}}$, with the fastest one moving at 84 $\mathrm{cm\,yr^{-1}}$ and the slowest one moving at 15 $\mathrm{cm\,yr^{-1}}$. They have a mean elevation of 3551 m and a mean size of 13 ha. We find no significant correlation between the flow speed and elevation or size of the rock glaciers. Their speeds are of the same order of magnitude as the flow speed of rock glaciers in other regions around the world, such as the European Alps (e.g. Berger et al., 2004; Delaloye et al., 2008, 2010; Lugon and Stoffel, 2010) and the Pyrenees (Serrano et al., 2006), Svalbard (Isaksen et al., 2000), and Wyoming, USA (Potter et al., 1998; Konrad et al., 1999), although none of these mapping efforts is as extensive and inclusive as this study.

Our complete regional survey reveals several important spatial patterns of rock glacier kinematics in the Sierra Nevada. Active rock glaciers tend to cluster to each other, implying a significant influence of regional conditions such as climate and topography on their locations. There is a spatial gap in the mountain areas near Mammoth

Lake where elevation is lower than 3000 m. Rock glaciers in the southern Sierra Nevada moved at a mean speed of 57 $cm\,yr^{-1}$, faster than the ones in the central Sierra Nevada whose mean speed was 39 $cm\,yr^{-1}$. This difference is largely due to the fact that the southern rock glaciers are higher in elevation and deeper in cirques. Another spatial contrast is that rock glacier speeds were less uniform in the southern area than in the central Sierra Nevada. Within some valleys in the southern area, such as the ones shown in Fig. 3, we observe a significant spatial variation in kinematic behaviors. It suggests strong influences of local physical factors such as slope, thickness, ice content, and hydrological conditions on surface speed.

We compare our inventory with the MW database in terms of rock glacier classes and locations. All of our identified active features fall into the cirque rock glacier class defined by Millar and Westfall (2008). However, only 14 (or 24 %) of them are collocated with the "active" ones in the MW database. Millar and Westfall (2008) used the term "active" based on the geomorphological and hydrological features, which may not all be actively moving. Our mapping method using InSAR is a direct measurement of surface flow motion and thus ensures that the identified targets are moving at a minimum speed of 10 $cm\,yr^{-1}$. In addition, 16 "active" cirque rock glaciers in the MW database are not included in our inventory because they are smaller than 2 ha. We exclude 12 of MW's "active" rock glaciers, for instance, 7 in the Piute Pass Glacier divide (37.23° N, 118.75° W), because they are either in the radar shadow zones or almost completely covered by ice. However, on the positive side, our inventory includes 44 active rock glaciers that not identified in the MW database from field work. For instance, within the region of Fig. 3, the MW database only includes one rock glacier (i.e. the South Fork rock glacier as shown in Fig. 3b). Overall, we conclude that our inventory based on InSAR and the MW database are complementary to each other; and together they provide a more complete and valuable dataset.

4.2 Surface flow of the Mount Gibbs rock glacier

In this subsection, we present the InSAR results on the surface flow at the Mount Gibbs rock glacier. We first show the spatial variability that is correlated with surface geomorphological features. We then provide a time series of surface flow speed showing its seasonal variation and its delay behind air temperature. Such a seasonal variability has not been observed previously using remote sensing methods.

On individual targets, InSAR provides a more spatially complete assessment of the surface flow than field measurements. Figure 4b shows the InSAR LOS speed over the Mount Gibbs rock glacier between 4 September 2007 and 5 December 2007. It clearly maps out two rapidly-flowing lobes (centered at "A" and "B") at speeds of $\sim 50\,\mathrm{cm\,yr^{-1}}$ starting from the middle section of the rock glacier. Along both lobes, InSAR LOS speed decreases towards the rock glacier snout. Such gradients in speed correlates well with surface ridges and furrows and suggest that these are geomorphological features caused by longitudinal compression. Figure 4b also shows rapid surface motion ($> 60\,\mathrm{cm\,yr^{-1}}$) near the head of the rock glacier (centered at "C"), although we cannot distinguish if this is motion of the glacier ice or rock debris. This InSAR map also reveals stable areas such as the southeast flank and the depression area between the two flowing branches. Other InSAR maps using different interferograms show a similar pattern but vary in magnitude.

Figure 5 shows a time series of surface speed at the marker "A" in Fig. 4b. Each triangle shows the mean downslope speed during the two consecutive PALSAR images in the same path, with the error bar showing the 1-σ uncertainty. The time series shows that the surface flow was slow in the spring, gradually increased throughout the summer, peaked in the fall at $48\,\mathrm{cm\,yr^{-1}}$, and then abruptly slowed in the winter, reaching to the minimum of $22\,\mathrm{cm\,yr^{-1}}$ in the following spring. This seasonal variation indicates a phase lag of ~ 3 months after the annual cycle of air temperature shown as the solid line in Fig. 5. We estimate the climatic air temperature at the rock glacier using the 1981–2010 mean air temperature records measured at Lee Vining (Fig. 1) and a temperature lapse rate of $-6.5\,^{\circ}\mathrm{C\,km}^{-1}$ (Lundquist and Cayan, 2007; Millar and Westfall, 2008) to account for the elevation difference. This estimated temperature is consistent with the field measurements (Millar et al., 2012) and the Parameter-elevation Regressions on Independent Slopes Model (PRISM) outputs (Daly et al., 1994).

5 Discussion

5.1 Strengths and weaknesses of InSAR-based rock glacier inventory

We have demonstrated that InSAR provides quantitative information on the surface flow of rock glaciers in a spatial scale of a major mountain range. The InSAR survey is unique: it quantifies rock glacier speed, which is difficult to measure in the field. Inventory mapping using InSAR is also more complete than optical studies that are limited by cloud covers. The InSAR survey is valuable: it reveals spatial patterns of rock glacier kinematics and provides benchmark information for studying the relationship between regional and local forcing conditions and rock glacier speed and for long-term monitoring efforts.

However, our InSAR-based inventory is still incomplete. Explained in Sect. 3.2, our inventory only includes rock glaciers that are larger than 2 ha, moving faster than $10\,\mathrm{cm\,yr}^{-1}$, flowing non-parallel to the satellite flight direction, and located outside radar layover (western slopes) or shadow zones. The lower bound on flow speed could be relaxed using interferograms spanning longer periods, provided that good coherence is maintained. The location constraints are not severe in the Sierra Nevada because most active rock glaciers are located on the eastern (leeward) slopes, where snow precipitation is substantially less than the western slopes. Realistically, in the Mount Gibbs rock glacier case, we find that snow cover in winters has little impact on the InSAR measurements, as the L-band radar waves can easily penetrate through thin and dry snow.

Discussion Paper | Discussion Paper | Discussion Paper | Discussion Paper |
TCD
7, 343–371, 2013
InSAR rock glaciers
Lin Liu et al.

Our InSAR-based flow speed estimates are not free of errors. Deformation signals in one interferogram are contaminated by decorrelation noises, atmospheric artifacts, and DEM errors. However, these errors are not correlated in time could be reduced using multiple interferograms. We may also over-estimate the annul rock glacier speeds by using late-summer interferograms, as the case study on the Mount Gibbs rock glacier suggests that the annual speed is likely smaller than the late-summer speed. Moreover, we introduce errors by assuming the same surface slope angle for all rock glaciers to simply the conversion from the InSAR LOS speed to downslope speed. This could be improved by carefully retrieving slopes from high-resolution DEM data.

5.2 Causes of seasonal variation in flow speed

According to the InSAR observations at the Mount Gibbs rock glacier (Fig. 5), seasonal variation of surface flow speed is significant, more than double from the minimum in the spring to the maximum in the fall. Our study adds one more finding to the few observations on seasonal variation of rock glacier speed (Haeberli, 1985; Arenson et al., 2002; Kääb et al., 2007; Perruchoud and Delaloye, 2007; Ikeda et al., 2008). Both the magnitude and the temporal delay of seasonal variability behind air temperature are comparable with the ground-based measurements at the Muragl (Arenson et al., 2002) and the Becs-de-Bosson rock glaciers (Perruchoud and Delaloye, 2007) in the Swiss Alps.

The exact cause(s) of the speed seasonal variations at the Mount Gibbs rock glacier is unclear. It might be partly due to the changes of rock glacier mechanical strength and rheology with ground temperature. We model the thermal diffusion of ground warming and the increase of the creep parameter of rock glacier materials using the same method of Kääb et al. (2007). Similar to Kääb et al.'s results, we find that the modeled seasonal variation in surface speed is approximately 5 % of the annual mean value, much smaller than the InSAR-observed 50 % variations. Even if we include a thin layer of highly deformable frozen material (Wagner, 1992; Arenson et al., 2002) in the flow model as done by Kääb et al. (2007), the seasonal variation is still less than 10 %.

Other possible mechanisms for seasonal variations include internal melting, basal sliding, and winter snow cover. Field investigations and water temperature measurements in the rock glacier talus outlet springs suggest persistent flow of water throughout the year (Millar et al., 2012). It takes time for temperature rising at depth to melt internal ice and for sufficient water to accumulate at the bottom of the rock glacier to act as a lubricant for basal sliding. Nonetheless, only a few studies have discussed the idea of basal sliding (Haeberli, 1985; Whalley and Martin, 1992) and it is unclear how commonly this mechanism occurs under rock glaciers. Ikeda et al. (2008) proposed that snowmelt water could infiltrate into the frozen debris and modulate surface motion of rock glaciers. However, their model predicts an increase in surface speed in early summer (May and June), different from our observations at the Mount Gibbs rock glacier. The delay of seasonal minimum speed that occurred in spring is likely caused by the refreezing of pore water and the winter snow cover, which insulates the ground from cold air and thus maintains surface speed. Modeling these mechanical and hydrological effects on rock glacier motion and its seasonal variation is a subject of future work.

5.3 Response of rock glaciers to climate warming: perspectives from InSAR

The kinematic response of rock glaciers to climate warming is contentious. The annual temperature in the Sierra Nevada is projected to rise by 2 to 4 °C by the end of the 21st century (Maurer, 2007). However, it is unclear whether rock glaciers will speed up due to accelerated degradation and melting and higher erosion rates (Gruber and Haeberli, 2007) or remain stable due to thermal insulation by the protective rock debris matrix (Clark et al., 1994; Barsch, 1996; Millar et al., 2012) and the local cooling effects caused by air circulation within rock matrix (Juliussen and Humlum, 2008; Leopold et al., 2011). Flow speed of some rock glaciers in the European Alps have accelerated in the last two decades or so (e.g. Kääb et al., 1997; Krainer and Mostler, 2000; Delaloye et al., 2008; Bodin et al., 2009). By contrast, in the Rocky Mountains of the USA, even observations longer than 30 yrs show no significant changes in rock glacier speed (Potter et al., 1998; Janke, 2005).

Practically, the ALOS PALSAR data are too short for monitoring long-terms changes in rock glacier flow as the satellite was in operation for only five years from late 2006 to early 2011. Nonetheless, our study strongly suggests the necessity of considering possible aliasing due to seasonal variation when estimating long-term changes in flow speed. Possible inter-annual variation in surface flow, which has been observed in the European Alps (Nöetzli and Vonder Müehll, 2010), further complicates the estimate of long-term trends. In general, it requires a long time series with high temporal sampling rates to separate possible long-term changes in rock glacier kinematics from seasonal and inter-annual variability. Other satellites such as ERS-1/2 and Envisat acquired longer time series of SAR data that are of potential for investigating response of rock glaciers in the Sierra Nevada to climate changes in the last two decades. The major challenge of using C-band data for rock glacier studies, however, is the problem of InSAR phase decorrelation due to fast surface flow. We suggest a strategy to form a long time series of interferograms that have short time spans (e.g. 35 days for ERS-1/2). The ERS-1/2 tandem (1-day intervals) and ice-phase (3-day intervals) data that are commonly used for ice glacier studies may not be useful because rock glacier motion within one day is of the order of 1 mm, too small to be reliably detected by InSAR. A few recently launched and future InSAR missions such as the TerraSAR-X, the Cosmo-Skymed, and the Sentinel Satellites will continue the observation period and provide denser temporal sampling rates (e.g. 11 days of TerraSAR-X) for monitoring rock glaciers.

6 Conclusions

In summary, we use InSAR data to compile an inventory of the flow speed, direction, and area of active motion at 59 rock glaciers in the Sierra Nevada. In the late summer of 2007, these rock glaciers moved at a mean speed of 55 $cm\,yr^{-1}$. Spatially, rock

TCD
7, 343–371, 2013

glaciers in the Southern Sierra Nevada moved faster than those in the central area. Our regional-scale InSAR study provides important baseline map of the kinematic states and useful guidance for field investigations and will be valuable for assessing the relationship of rock glaciers flow with regional climate and local conditions.

We also conduct a detailed InSAR study to map the surface flow of the Mount Gibbs rock glacier. We find two fast-moving branches in the lower part of the rock glacier, collocated with surface flow lines. More interestingly, we observe a significant seasonal variability of surface speed, more than double in the fall from its minimum in the spring. Our findings suggest the necessity of a long time series with dense sampling to separate long-terms changes in rock glacier kinematics associated with climate change from seasonal variations.

Supplementary material related to this article is available online at: http://www.the-cryosphere-discuss.net/7/343/2013/tcd-7-343-2013-supplement.zip.

Acknowledgements. The ALOS PALSAR data are copyrighted by the Japan Aerospace Exploration Agency and provided by the Alaska Satellite Facility, University of Alaska Fairbanks. Climatic data at Lee Vining, CA are provided by the Western Regional Climate Center, NOAA. This research was supported primarily by the George Thompson Postdoctoral Fellowship to Lin Liu from the Department of Geophysics, Stanford University. Matlab and Generic Mapping Tools (Wessel and Smith, 1998) were used to make the figures.

References

Arenson, L., Hoelzle, M., and Springman, S.: Borehole deformation measurements and internal structure of some rock glaciers in Switzerland, Permafrost Periglac., 13, 117–135, doi:10.1002/ppp.414, 2002. 356

Avian, M., Kellerer-Pirklbauer, A., and Bauer, A.: LiDAR for monitoring mass movements in permafrost environments at the cirque Hinteres Langtal, Austria, between 2000 and 2008, Nat. Hazards Earth Syst. Sci., 9, 1087–1094, doi:10.5194/nhess-9-1087-2009, 2009. 345

Barsch, D.: Nature and importance of mass-wasting by rock glaciers in alpine permafrost environments, Earth Surf. Processes, 2, 231–245, doi:10.1002/esp.3290020213, 1977. 344

Barsch, D.: Rockglaciers: Indicators for the Present and Former Geoecology in High Mountain Environments, Springer, Berlin, 1996. 345, 357

Berardino, P., Fornaro, G., Lanari, R., and Sansosti, E.: A new algorithm for surface deformation monitoring based on small baseline differential SAR interferograms, IEEE T. Geosci. Remote, 40, 2375–2383, doi:10.1109/TGRS.2002.803792, 2002. 350

Berger, J., Krainer, K., and Mostler, W.: Dynamics of an active rock glacier (Ötztal Alps, Austria), Quaternary Res., 62, 233–242, doi:10.1016/j.yqres.2004.07.002, 2004. 352

Berthling, I., Etzelmüller, B., Eiken, T., and Sollid, J. L.: Rock glaciers on Prins Karls Forland, Svalbard. I: internal structure, flow velocity and morphology, Permafrost Periglac., 9, 135–145, doi:10.1002/(SICI)1099-1530(199804/06)9:2<135::AID-PPP284>3.0.CO;2-R, 1998. 345

Bodin, X., Thibert, E., Fabre, D., Ribolini, A., Schoeneich, P., Francou, B., Reynaud, L., and Fort, M.: Two decades of responses (1986–2006) to climate by the Laurichard rock glacier, French Alps, Permafrost Periglac., 20, 331–344, doi:10.1002/ppp.665, 2009. 357

Brenning, A.: Geomorphological, hydrological and climatic significance of rock glaciers in the Andes of Central Chile (33–35° S), Permafrost Periglac., 16, 231–240, doi:10.1002/ppp.528, 2005. 344, 345

Burger, K. C., Degenhardt Jr., J. J., and Giardino, J. R.: Engineering geomorphology of rock glaciers, Geomorphology, 31, 93–132, doi:10.1016/S0169-555X(99)00074-4, 1999. 345

Chen, C. and Zebker, H.: Phase unwrapping for large SAR interferograms: statistical segmentation and generalized network models, IEEE T. Geosci. Remote, 40, 1709–1719, doi:10.1109/TGRS.2002.802453, 2002. 349

Clark, D. H. and Gillespie, A. R.: Timing and significance of Late-glacial and Holocene cirque glaciation in the Sierra Nevada, California, Quatern. Int., 38–39, 21–38, doi:10.1016/S1040-6182(96)00024-9, 1997. 347

Clark, D. H., Clark, M. M., and Gillespie, A. R.: Debris-covered glaciers in the Sierra Nevada, California, and their implications for snowline reconstructions, Quaternary Res., 41, 139–153, doi:10.1006/qres.1994.1016, 1994. 345, 357

Croce, F. A. and Milana, J. P.: Internal structure and behaviour of a rock glacier in the Arid Andes of Argentina, Permafrost Periglac., 13, 289–299, doi:10.1002/ppp.431, 2002. 345

Daly, C., Neilson, R. P., and Phillips, D. L.: A statistical-topographic model for mapping climatological precipitation over mountainous terrain, J. Appl. Meteorol., 33, 140–158, doi:10.1175/1520-0450(1994)033<0140:ASTMFM>2.0.CO;2, 1994. 355

Degenhardt Jr., J. J.: Development of tongue-shaped and multilobate rock glaciers in alpine environments – interpretations from ground penetrating radar surveys, Geomorphology, 109, 94–107, doi:10.1016/j.geomorph.2009.02.020, 2009. 344

Delaloye, R., Perruchoud, E., Avian, M., Kaufmann, V., Bodin, X., Hausmann, H., Ikeda, A., Kääb, A., Kellerer-Pirklbauer, A., Krainer, K., et al.: Recent Interannual variations of rock-glaciers creep in the European Alps, in: Proceedings of the 9th International Conference on Permafrost, Fairbanks, Alaska, 2008. 345, 352, 357

Delaloye, R., Lambiel, C., and Gärtner-Roer, I.: Overview of rock glacier kinematics research in the Swiss Alps: seasonal rhythm, interannual variations and trends over several decades, Geogr. Helv., 65, 135–145, 2010. 346, 352

Gesch, D., Oimoen, M., Greenlee, S., Nelson, C., Steuck, M., and Tyler, D.: The national elevation dataset, Photogramm. Eng. Rem. S., 68, 5–11, 2002. 349

Gruber, S. and Haeberli, W.: Permafrost in steep bedrock slopes and its temperature-related destabilization following climate change, J. Geophys. Res., 112, F02S18, doi:10.1029/2006JF000547, 2007. 357

Haeberli, W.: Creep of mountain permafrost: internal structure and flow of alpine rock glaciers, Mit. Vers. Was., 77, 5–142, 1985. 356, 357

Haeberli, W., Kääb, A., Wagner, S., Mühll, D., Geissler, P., Haas, J., Glatzel-Mattheier, H., and Wagenbach, D.: Pollen analysis and ^{14}C age of moss remains in a permafrost core recovered from the active rock glacier Murtèl-Corvatsch, Swiss Alps: geomorphological and glaciological implications, J. Glaciol., 45, 1–8, 1999. 345

Harrison, S., Whalley, B., and Anderson, E.: Relict rock glaciers and protalus lobes in the British Isles: implications for Late Pleistocene mountain geomorphology and palaeoclimate, J. Quaternary Sci., 23, 287–304, doi:10.1002/jqs.1148, 2008. 345

Humlum, O.: The climatic significance of rock glaciers, Permafrost Periglac., 9, 375–395, doi:10.1002/(SICI)1099-1530(199810/12)9:4<375::AID-PPP301>3.0.CO;2-0, 1998. 345

Humlum, O.: The geomorphic significance of rock glaciers: estimates of rock glacier debris volumes and headwall recession rates in West Greenland, Geomorphology, 35, 41–67, doi:10.1016/S0169-555X(00)00022-2, 2000. 344

Ikeda, A., Matsuoka, N., and Kääb, A.: Fast deformation of perennially frozen debris in a warm rock glacier in the Swiss Alps: an effect of liquid water, J. Geophys. Res., 113, F01021, doi:10.1029/2007JF000859, 2008. 356, 357

Isaksen, K., Ødegård, R. S., Eiken, T., and Sollid, J. L.: Composition, flow and development of two tongue-shaped rock glaciers in the permafrost of Svalbard, Permafrost Periglac., 11, 241–257, doi:10.1002/1099-1530(200007/09)11:3<241::AID-PPP358>3.0.CO;2-A, 2000. 352

Janke, J.: Long-term flow measurements (1961–2002) of the Arapaho, Taylor, and Fair rock glaciers, Front Range, Colorado, Phys. Geogr., 26, 313–336, doi:10.2747/0272-3646.26.4.313, 2005. 358

Juliussen, H. and Humlum, O.: Thermal regime of openwork block fields on the mountains Elgåhogna and Sølen, central-eastern Norway, Permafrost Periglac., 19, 1–18, doi:10.1002/ppp.607, 2008. 357

Kääb, A.: Monitoring high-mountain terrain deformation from repeated air- and spaceborne optical data: examples using digital aerial imagery and ASTER data, ISPRS J. Photogramm., 57, 39–52, doi:10.1016/S0924-2716(02)00114-4, 2002. 345

Kääb, A., Haeberli, W., and Gudmundsson, G. H.: Analysing the creep of mountain permafrost using high precision aerial photogrammetry: 25 years of monitoring Gruben rock glacier, Swiss Alps, Permafrost Periglac., 8, 409–426, doi:10.1002/(SICI)1099-1530(199710/12)8:4<409::AID-PPP267>3.0.CO;2-C, 1997. 345, 357

Kääb, A., Frauenfelder, R., and Roer, I.: On the response of rockglacier creep to surface temperature increase, Global Planet. Change, 56, 172–187, doi:10.1016/j.gloplacha.2006.07.005, 2007. 356

Kenyi, L. and Kaufmann, V.: Estimation of rock glacier surface deformation using SAR interferometry data, IEEE T. Geosci. Remote, 41, 1512–1515, doi:10.1109/TGRS.2003.811996, 2003. 346

Kistler, R. W.: Geologic map of the Mono Craters quadrangle, Mono and Tuolumne counties, California, Map GQ-462, Tech. rep., US Geological Survey, 1966. 348

Konrad, S. K., Humphrey, N. F., Steig, E. J., Clark, D. H., Potter, N., and Pfeffer, W. T.: Rock glacier dynamics and paleoclimatic implications, Geology, 27, 1131–1134, 1999. 345, 352

Krainer, K. and Mostler, W.: Reichenkar rock glacier: a glacier derived debris-ice system in the western Stubai Alps, Austria, Permafrost Periglac., 11, 267–275, doi:10.1002/1099-1530(200007/09)11:3<267::AID-PPP350>3.0.CO;2-E, 2000. 345, 357

Lambiel, C. and Delaloye, R.: Contribution of real-time kinematic GPS in the study of creeping mountain permafrost: examples from the Western Swiss Alps, Permafrost Periglac., 15, 229–241, doi:10.1002/ppp.496, 2004. 345

Leopold, M., Williams, M., Caine, N., Völkel, J., and Dethier, D.: Internal structure of the Green Lake 5 rock glacier, Colorado Front Range, USA, Permafrost Periglac., 22, 107–119, doi:10.1002/ppp.706, 2011. 357

Lugon, R. and Stoffel, M.: Rock-glacier dynamics and magnitude-frequency relations of debris flows in a high-elevation watershed: Ritigraben, Swiss Alps, Glob. Planet. Change, 73, 202–210, doi:10.1016/j.gloplacha.2010.06.004, 2010. 352

Lundquist, J. D. and Cayan, D. R.: Surface temperature patterns in complex terrain: daily variations and long-term change in the central Sierra Nevada, California, J. Geophys. Res., 112, D11124, doi:10.1029/2006JD007561, 2007. 355

Maurer, E.: Uncertainty in hydrologic impacts of climate change in the Sierra Nevada, California, under two emissions scenarios, Climatic Change, 82, 309–325, doi:10.1007/s10584-006-9180-9, 2007. 357

Millar, C. I. and Westfall, R. D.: Rock glaciers and related periglacial landforms in the Sierra Nevada, CA, USA; inventory, distribution and climatic relationships, Quatern. Int., 188, 90–104, doi:10.1016/j.quaint.2007.06.004, available at: http://nsidc.org/data/ggd652.html, 2008. 346, 347, 353, 355, 366

Millar, C. I., Westfall, R. D., and Delany, D. L.: Thermal and hydrologic attributes of rock glaciers and periglacial talus landforms, Sierra Nevada, California, USA, Quatern. Int., doi:10.1016/j.quaint.2012.07.019, in press, 2012. 345, 355, 357

Nagler, T., Mayer, C., and Rott, H.: Feasibility of DINSAR for mapping complex motion fields of alpine ice- and rock-glaciers, in: Retrieval of Bio- and Geo-Physical Parameters from SAR Data for Land Applications, edited by: Wilson, A. and Quegan, S., Vol. 475 of ESA Special Publication, 377–382, 2002. 346

Nöetzli, J. and Vonder Müehll, D. (Eds.): Permafrost in Switzerland 2006/2007 and 2007/2008, Glaciological Report (Permafrost), The Cryospheric Commission of the Swiss Academy of Sciences, 2010. 345, 358

Perruchoud, E. and Delaloye, R.: Short-term changes in surface velocities on the Becs-de-Bosson rock glacier (western Swiss Alps), in: Proceedings of the 9th International Symposium on High Mountain Remote Sensing Cartography (HMRSC-IX), vol. 43, 14–15, 2007. 356

Potter, N. J., Steig, E. J., Clark, D. H., Speece, M. A., Clark, G. M., and Updike, A. B.: Galena Creek rock glacier revisited: new observations on an old controversy, Geogr. Ann. A, 80, 251–265, 1998. 352, 358

Rignot, E., Hallet, B., and Fountain, A.: Rock glacier surface motion in Beacon Valley, Antarctica, from synthetic-aperture radar interferometry, Geophys. Res. Lett., 29, 1607, doi:10.1029/2001GL013494, 2002. 346

Rott, H. and Siegel, A.: Analysis of mass movements in alpine terrain by means of SAR interferometry, in: Geoscience and Remote Sensing Symposium, 1999, IGARSS '99 Proceedings, IEEE 1999 International, vol. 4, 1933–1936, doi:10.1109/IGARSS.1999.774991, 1999. 346

Serrano, E., San Jose, J., and Agudo, C.: Rock glacier dynamics in a marginal periglacial high mountain environment: flow, movement (1991–2000) and structure of the Argualas rock glacier, the Pyrenees, Geomorphology, 74, 285–296, doi:10.1016/j.geomorph.2005.08.014, 2006. 352

Strozzi, T., Kääb, A., and Frauenfelder, R.: Detecting and quantifying mountain permafrost creep from in situ inventory, space-borne radar interferometry and airborne digital photogrammetry, Int. J. Remote Sens., 25, 2919–2931, doi:10.1080/0143116042000192330, 2004. 346

Wagner, S.: Creep of alpine permafrost, investigated on the murtel rock glacier, Permafrost Periglac., 3, 157–162, doi:10.1002/ppp.3430030214, 1992. 356

Wahrhaftig, C. and Cox, A.: Rock glaciers in the Alaska range, Geol. Soc. Am. Bull., 70, 383–436, 1959. 345

Wessel, P. and Smith, W. H. F.: New, improved version of generic mapping tools released, EOS T. Am. Geophys. Un., 79, 579–579, doi:10.1029/98EO00426, 1998. 359

Whalley, W. B. and Martin, H. E.: Rock glaciers: II Models and mechanisms, Prog. Phys. Geogr., 16, 127–186, 1992. 357

Zebker, H., Hensley, S., Shanker, P., and Wortham, C.: Geodetically Accurate InSAR Data Processor, IEEE T. Geosci. Remote, 48, 4309–4321, doi:10.1109/TGRS.2010.2051333, 2010. 349

Table 1. Interferograms made from the case study on the Mount Gibbs rock glacier. Names of interferograms are in the format "yyyymmdd–yyyymmdd", after the dates of the two SAR scenes used. Column "B perp" lists the perpendicular baselines of the interferograms.

Interferogram	Timespan (days)	B perp (m)	Path/Frame
20070402–20070518	46	–286	216/750
20070402–20070703	92	92	216/750
20070402–20070818	138	315	216/750
20070518–20070703	46	378	216/750
20070518–20070818	92	601	216/750
20070703–20070818	46	223	216/750
20070904–20071205	92	349	217/740
20071003–20080103	92	354	216/750
20071020–20071205	46	109	217/740
20071020–20080120	92	534	217/740
20071205–20080120	46	424	217/740
20080103–20080520	92	1218	216/750

TCD
7, 343–371, 2013

Table 2. Summary of the active rock glaciers in the Sierra Nevada based on InSAR and comparisons with the "active" cirque rock glaciers in the Millar and Westfall (2008) (MW) database. The term "active" used by the MW database is based on the geomorphological and hydrological features.

	InSAR	MW
Number	59	67
Mean elevation (m)	3551	3390
Elevation range (m)	3077–3787	2673–3901
Mean size (ha)	13	20
Size range (ha)	3–46	N/A
Mean length (m)	624	N/A
Mean width (m)	201	N/A
Mean length-to-width ratio	3.3	N/A
Mean flow speed ($cm\,yr^{-1}$)	55	N/A
Flow speed range ($cm\,yr^{-1}$)	15–84	N/A

TCD
7, 343–371, 2013

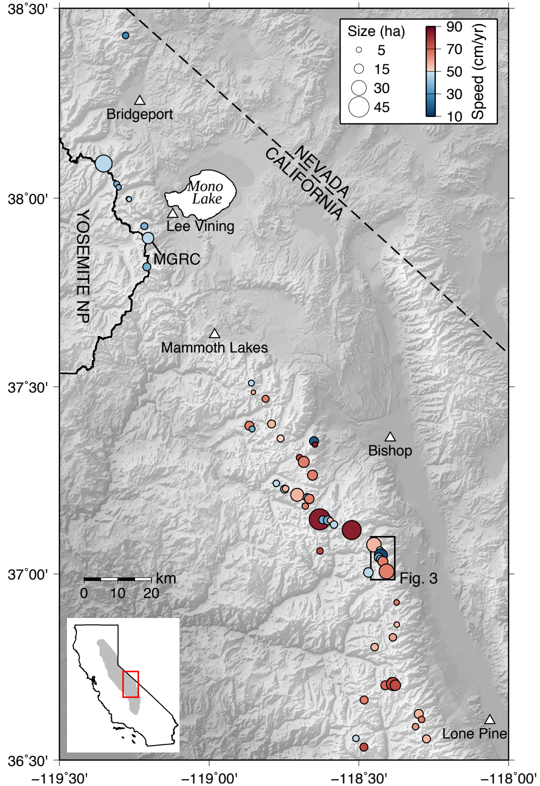

Fig. 1. Map of the study area in the central Sierra Nevada of California, USA. Circles are active rock glaciers based on our InSAR measurements. The size and color of the circles represent the size and speed of the rock glaciers, respectively. "MGRC" stands for the Mount Gibbs Rock Glacier. The black box outlines the area shown in Fig. 3. The inset map of California shows the Sierra Nevada in gray and the location of the study area as a red box.

TCD
7, 343–371, 2013

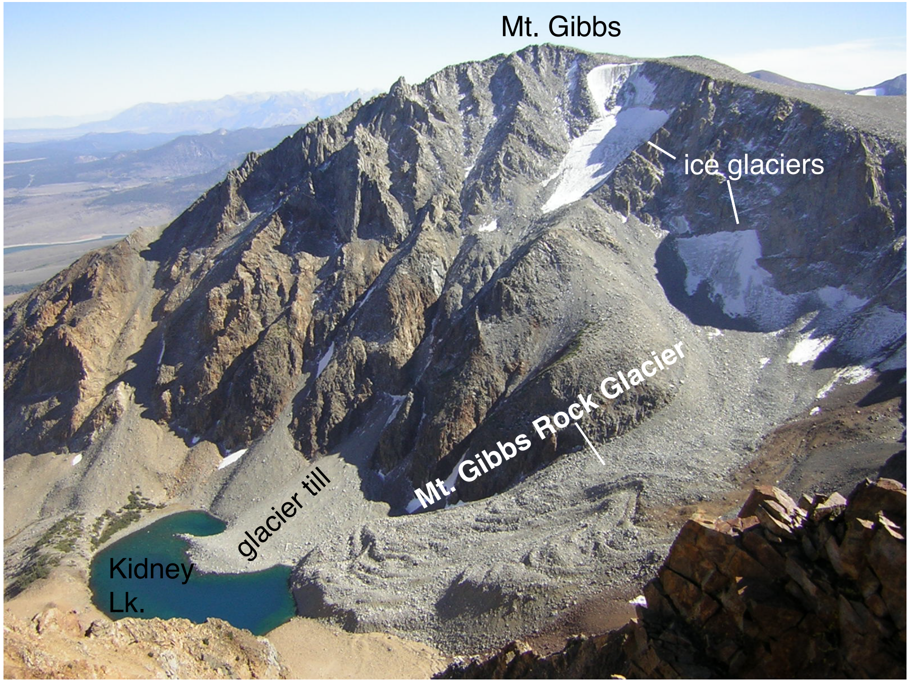

Fig. 2. The Mount Gibbs rock glacier from the shoulder of Mount Dana looking south (Photo: C. Millar).

TCD
7, 343–371, 2013

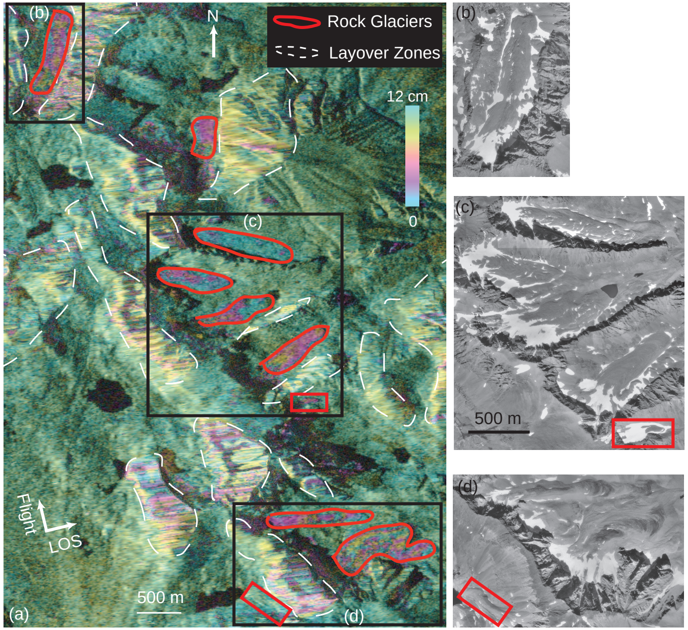

Fig. 3. (a) Wrapped and geocoded PALSAR interferogram spanning 18 August 2007 to 3 October 2007 (Path 216, Frame 730). Background is the radar intensity image. Actively-moving areas of rock glaciers are outlined by red polygons. Red boxes outline two rock glaciers not included in our inventory (see Sect. 3.2). White dashed polygons outline radar layover zones. Satellite flight and line-of-sight (LOS) directions are plotted as perpendicular vectors. **(b–d)** are aerial photos of the areas defined in **(a)**. These photos were taken in late summer of 1998 and produced by the USDA Geospatial Service and Technology Center. All photos are to the same scale shown in **(c)**.

TCD
7, 343–371, 2013

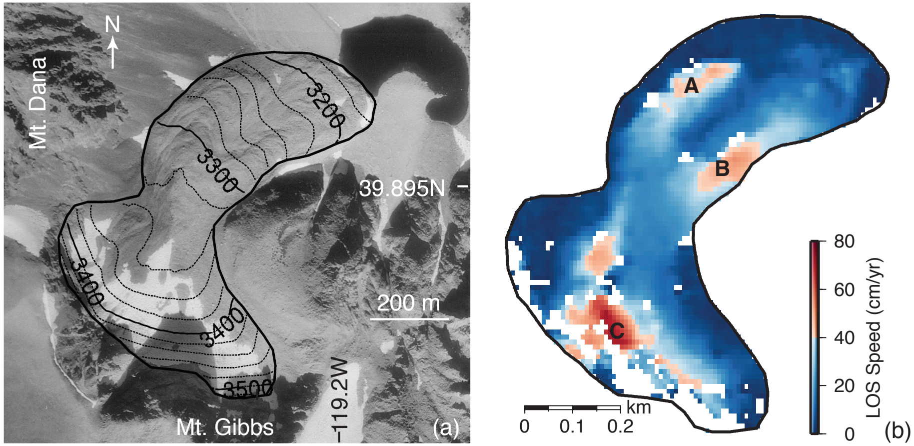

Fig. 4. (a) Aerial photo of the Mount Gibbs rock glacier, taken on 25 September 1993. Rock glacier boundary is roughly outlined by the solid black line. Dashed lines are topographic contours spaced at 20 m. **(b)** InSAR line-of-sight speed during 4 September 2007 and 5 December 2007. White areas within the black boundary are places of low interferometric coherence. “A”, “B”, and “C” mark the center of fast-moving areas.

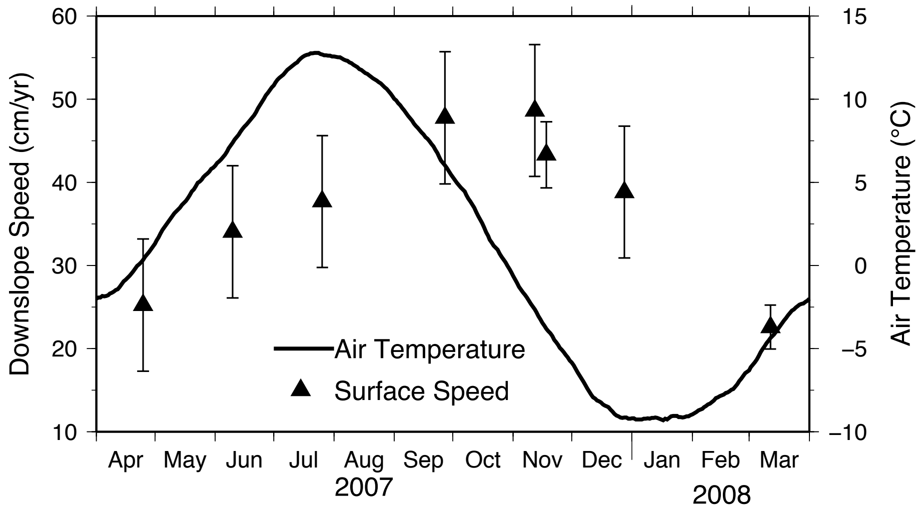

Fig. 5. Time series of the estimated air temperature (solid line) and the InSAR-measured downslope speed (triangles) at the marker "A" shown in Fig. 4b. The error bars are the 1-σ uncertainties of the measured speed.

TCD
7, 343–371, 2013